Microwave Spectroscopic Imaging of the Magnetic Reconnection Region in the 2017 September 10 Eruptive Solar Flare

Bin Chen[1], Dale E. Gary[1], Gregory D. Fleishman[1], Säm Krucker[2], Gelu M. Nita[1], Brian R. Dennis[3], Sijie Yu[1], Natsuha Kuroda[1], Katharine Reeves[4], Vanessa Polito[4], Albert Y Shih[3]

[1]New Jersey Institute of Technology, [2]UC Berkeley, [3]NASA Goddard Space Flight Center, [4]Havard-Smithsonian Center for Astrophysics

Abstract

The newly commissioned Expanded Owens Valley Solar Array (EOVSA) obtained excellent high-cadence (1 s), microwave spectroscopic imaging of the spectacular eruptive solar flare on 2017 September 10 in 2.5–18 GHz. During the early impulsive phase of the flare (~15:53–15:55 UT), EOVSA images reveal an elongated microwave (MW) source that connects the top of the cusp-shaped flare arcade to the bottom of the erupting magnetic flux rope. The spatially resolved spectra of this microwave source show characteristics of gyrosynchrotron radiation, suggesting the presence of high-energy nonthermal electrons throughout the source region that presumably encloses the magnetic reconnection site(s) and bi-directional reconnection outflows. In addition, the lower and upper portions of the source seem to have different spatial and spectral properties. We discuss their implications in magnetic energy release and electron acceleration.

The EOVSA

Frequency range	2.5–18 GHz (now 1–18 GHz)	**Correlator inputs**	16 x 2 poln
Data channels	2 (dual polarization)	**Number and type of antennas**	Thirteen 2.1-m antennas One 27-m (cal. only)
IF bandwidth	500 MHz single sideband	**System Temperature**	570 K (2m); <100 K (27m)
Frequency resolution	500 MHz band 134 science channels (current)	**Array Size and # of Baselines**	1.1 km EW x 1.2 km NS; 78 baselines
Time resolution	Sample time: 20 ms Full Sweep: 1 s	**Angular resolution**	$56''/n_{GHz} \times 51''/n_{GHz}$

Event Overview

- EOVSA obtained excellent microwave imaging spectroscopy observations of SOL2017-09-10, a classic partially-occulted solar limb flare associated with an erupting magnetic flux rope.
- This event is also well-covered in hard X-rays (HXRs) and gamma-rays by RHESSI and Fermi LAT/GBM (Omodei et al 2018), in EUV by SDO/AIA (Yan et al 2018), the Solar Ultraviolet Imager (SUVI) aboard GOES-R (Seaton et al. 2017), Hinode/EIS (Warren et al. 2017), and partially covered by IRIS (Reeves et al. 2018, poster #306.104).
- An overview of EOVSA observations of this event is presented in Gary et al. 2018 (see Gary's talk 315.01, Wed 14:00-14:25).

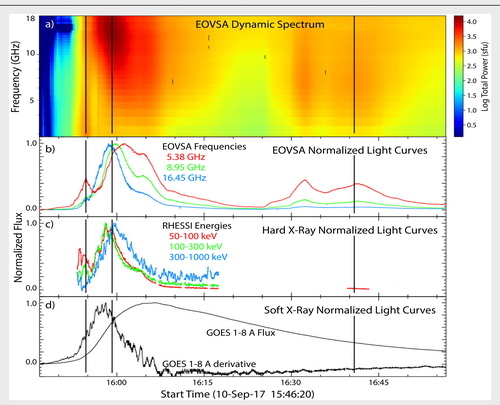

Figure 1. Microwave dynamic spectrum and normalized light curves of the first ~1 hour of the event at different wavelengths. **a)** EOVSA total power dynamic spectrum from 2.5-18 GHz, with colors representing the flux density in sfu. **b)** Normalized time profiles of the MW emission at three frequencies. **c)** Normalized time profiles of RHESSI HXR counts, with a gap due to passage of the spacecraft through the SAA. **d)** Normalized GOES 1-8 Å flux and time derivative. (From Gary et al. 2018.)

The Early Impulsive Phase

- The early impulsive phase is characterized by an initial peak in MW and HXR at ~15:54 UT (Figure 1, leftmost vertical line), when the magnetic flux rope undergoes a transition from slow rise to fast eruption (Fig. 2).
- EOVSA was capable of imaging the entire flaring region with excellent dynamic range (~20:1) for all its frequency bands. Figure 3a shows the multi-frequency MW images at 30 bands in 3.4–17.9 GHz. Fig. 3b-c shows a more detailed view, when the flux rope body and the underlying current-sheet like feature are both clearly seen.
- An over-the-looptop source is seen in HXRs (white contours in Fig. 3b-c), coinciding with the high-frequency MW source.
- MW emission is more complex at the low frequencies and fills a much larger area of the flaring region.

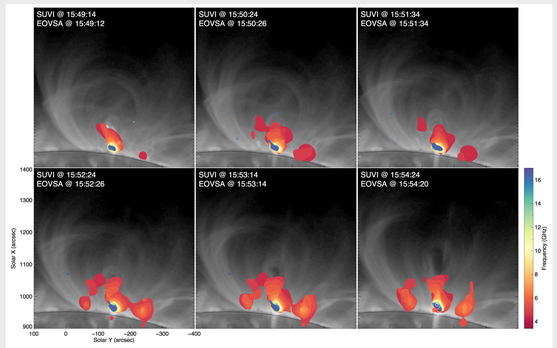

Figure 2. EOVSA multi-frequency images during the early impulsive phase from 15:49:14 to 15:54:20 UT, shown as filled 20% contours of MW emission at 28 spectral windows, with hues indicated in the color bar. Background is the corresponding GOES-R/SUVI 195 Å EUV images (in grayscale of log intensity).

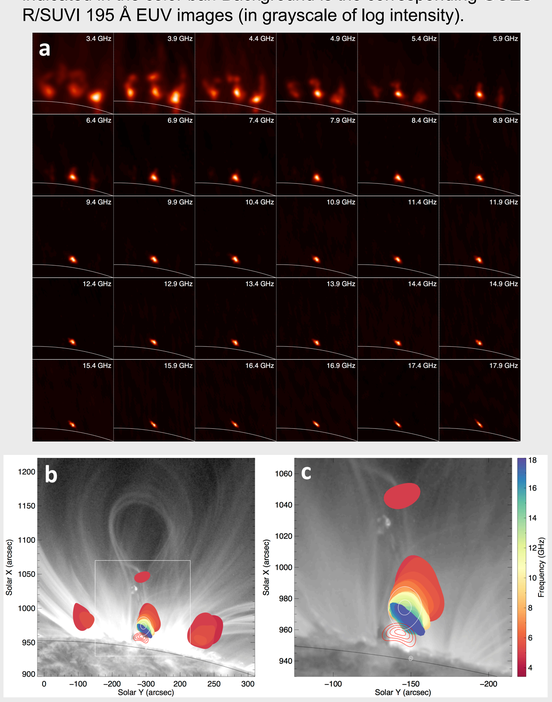

Figure 3. **a**) EOVSA multi-frequency images during the early impulsive phase at 15:54:20 UT in 3.4–17.9 GHz. **b**) EOVSA and RHESSI images overlaid on AIA 171 Å EUV image. EOVSA images are shown with filled 50% contours at all 30 spectral windows, with hues shown in the color bar. Red contours are RHESSI 12–18 keV soft X-ray image, showing the hot flaring arcade. White contours show the over-the-loop-top hard X-ray source (RHESSI 30–100 keV). **c**) Enlarged view of panel b. The field of view is shown as a white box in b.

MW Spectral Imaging of Magnetic Reconnection Region

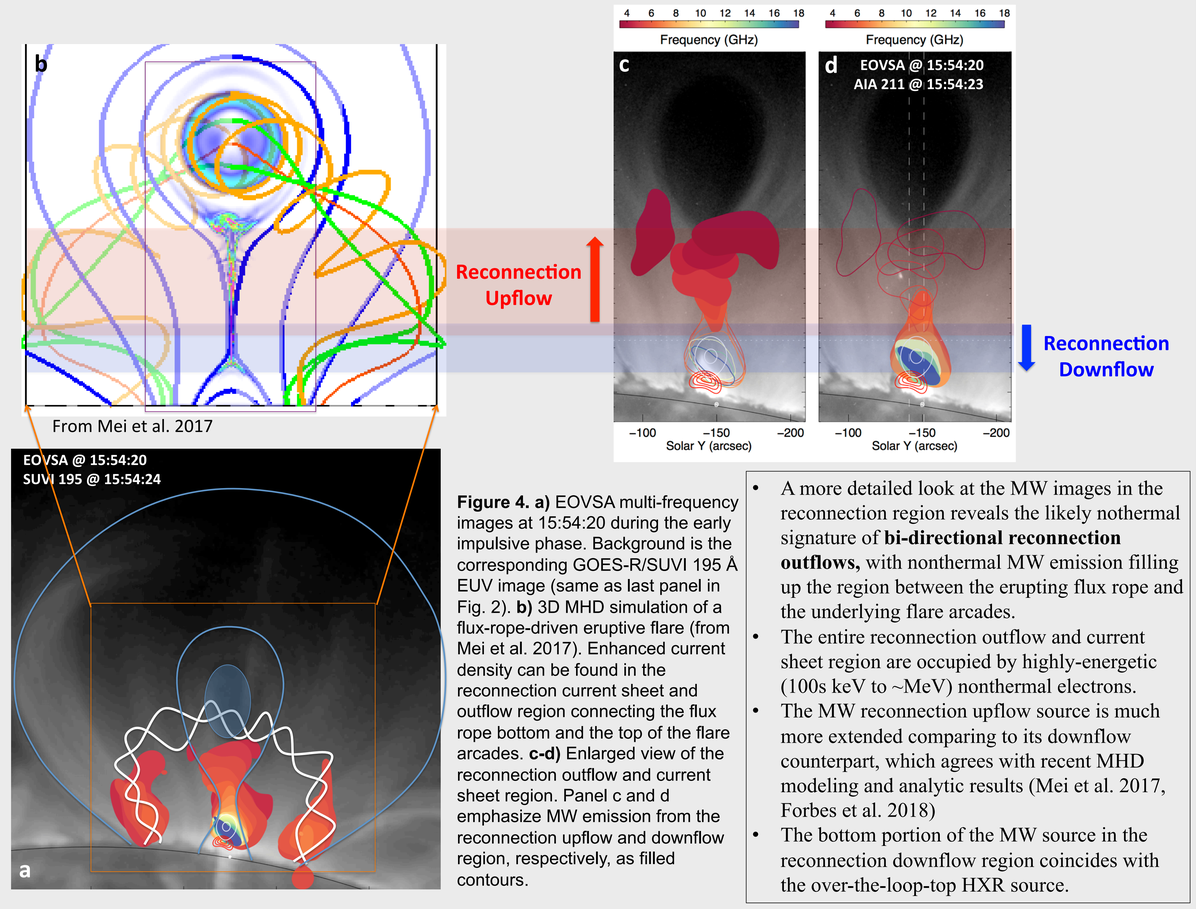

Figure 4. a) EOVSA multi-frequency images at 15:54:20 during the early impulsive phase. Background is the corresponding GOES-R/SUVI 195 Å EUV image (same as last panel in Fig. 2). **b)** 3D MHD simulation of a flux-rope-driven eruptive flare (from Mei et al. 2017). Enhanced current density can be found in the reconnection current sheet and outflow region connecting the flux rope bottom and the top of the flare arcades. **c-d)** Enlarged view of the reconnection outflow and current sheet region. Panel c and d emphasize MW emission from the reconnection upflow and downflow region, respectively, as filled contours.

- A more detailed look at the MW images in the reconnection region reveals the likely nothermal signature of **bi-directional reconnection outflows,** with nonthermal MW emission filling up the region between the erupting flux rope and the underlying flare arcades.
- The entire reconnection outflow and current sheet region are occupied by highly-energetic (100s keV to ~MeV) nonthermal electrons.
- The MW reconnection upflow source is much more extended comparing to its downflow counterpart, which agrees with recent MHD modeling and analytic results (Mei et al. 2017, Forbes et al. 2018)
- The bottom portion of the MW source in the reconnection downflow region coincides with the over-the-loop-top HXR source.

Current Sheet: MW Spectra

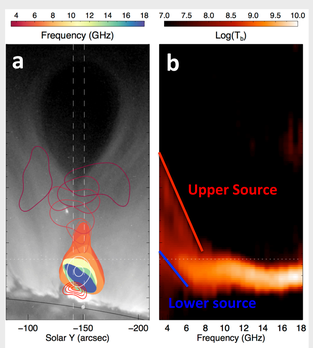

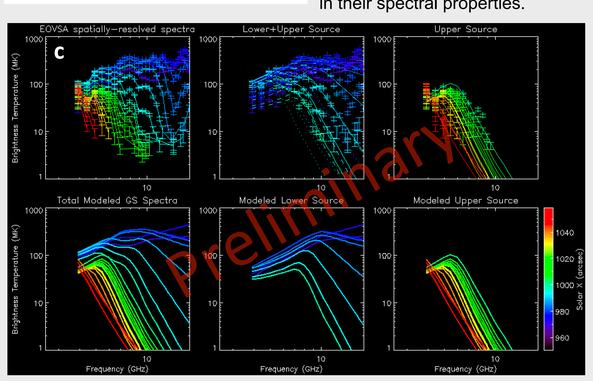

Figure 5. a) MW images at 15:54:20. **b)** MW "frequency-distance" map. This is analogue to the time-distance maps, but the horizontal axis shows frequency instead. Each horizontal slice in the map represents the MW spectrum (red-temperature color) obtained at a certain height along the current sheet (dashed lines in panel a). The corresponding brightness spectra are shown in **c**, with blue to red colors representing increasing height. Top and bottom rows show the observed and fit MW spectra based on gyrosynchrotron radiation. The lower and upper source (middle and right panels) are notably different in their spectral properties.

Concluding Remarks

- EOVSA observations reveal a **nonthermal view** of the **entire reconnection outflow and current sheet region** from the bottom of the flux rope to the top of the flaring arcades.
- **The reconnection outflow and current sheet region are filled with mildly-relativistic electrons.**
- The bottom portion of the MW source in the reconnection downflow region coincides with the over-the-loop-top HXR source, while the MW reconnection upflow source is much more extended.
- More detailed investigation based on the spatially-resolved MW spectra is ongoing, which may provide important insights on electron acceleration and transport.

References

Forbes et al. 2018, *ApJ*, 858, 70
Gary et al. 2018, "Microwave and Hard X-Ray Observations of the 2017 Sep 10 Solar Limb Flare," *ApJ*, submitted
Mei et al. 2017, *A&A*, 604, 7
Seaton & Darnel 2018, *ApJ*, 852, 9
Omodei et al. 2018, arXiv: 1803.07654
Warren et al. 2018, *ApJ*, 854, 122
Yan et al. 2018, *ApJ*, 853, 18

Acknowledgements

The authors appreciate data made available by the SDO/AIA and GOES-R/SUVI teams. This work is supported by NSF grants AST-1615807, AST-1735405, AGS-1654382, AGS-1723436, AGS-1817277 and NASA grants NNX14AK66G, 80NSSC18K0015, NNX17AB82G, NNX14AC87G, and 80NSSC18K0667 to NJIT. The RHESSI related part of this work is supported by NASA contract NAS 5-98033.